

## Landslide run-out derived from LiDAR micro-topography and numerical modeling: Route 9, Dakeng bridge watershed

Wei-Kai Huang<sup>(1)</sup>, Ching-Fang Lee<sup>(1)</sup>, Lun-Wei Wei<sup>(1)</sup>, Yu-Lin Chang<sup>(1)</sup>,  
Shu-Yeong Chi<sup>(1)</sup>

(1) Disaster Prevention Technology Research Center, Sinotech Engineering Consultants, INC.  
(Taipei 115, Taiwan, R.O.C.)  
E-mail: wuangwk@sinotech.org.tw

### Abstract

High resolution digital elevation data acquired from LiDAR scanning is used to interpret the micro-topography of the Dakeng bridge watershed, an area crossed by Route 9 in Taiwan that is frequented by natural disasters. In addition to identifying the extent of potentially unstable areas within the watershed, an empirical model based on disaster records of landslide volume and area is employed to estimate resultant landslide volume. That volume is then input into Particle Flow Code (PFC3D<sup>TM</sup>) to model the landslide failure process and run-out.

Results reveal that the Dakeng bridge watershed is marked by several clear tension cracks, head scarps and gravitationally deformed areas. The total gravitationally deformed area is 5.9 ha. The landslide volume resulting from the gravitationally deformed area is 324,490 m<sup>3</sup> and the landslide run-out includes the confluence of the watershed where deposits may be as much as 13 m and cause the formation of a landslide dam. In the future, rapid stream aggradation or scour effect may occur in the area downstream of this deposit.

**Keywords: Micro-topography, LiDAR, Discrete Element Method, Landslide run-out**

### 1. Introduction

Route 9, also known as the Su-Hua highway, is the primary transportation route along the east coast of Taiwan. As a result of heavy typhoon rains during recent years, the highway has frequently been severed by debris flows and landslides. According to the Ministry of Transportation and Communication (MOTC) Highway Disaster Information System, regarding disasters along Route 9 between Suao and Dongao between 2009 to 2013, slope-land disasters were most frequent during 2010 Typhoon Megi. Additionally, according to Central Weather Bureau precipitation records, Typhoon Megi affected the Suao area between October 19th and October 21st, 2010 dropping a total of 939 mm of rain with rainfall intensities was as high as 121 mm/hr(10/21, 13:00-14:00). In addition to setting precipitation records, Typhoon Megi also triggered several landslides between Suao and Nanao that severed both lanes of Route 9 and ensnared a tour bus in debris, pushing it off the highway and into the ocean (Central Geologic Bureau, 2011; Lee, 2010).

Lai (1986) divided the stretch of Route 9

between Suao and Chongde into 15 unique geologic zones. In addition to performing field experiments and noting outcrop orientation, exposed rock was also evaluated using a rock mass rating (RMR) and the Q system and physical experiments were carried out on the slope material in order to assess the stability and the failure mode of the slope. Results revealed that the primary failure mode is toppling and wedge failure. Chu et al. (2013) used Midas GTS finite element analysis software to create a model of the Su-Hua highway 115.9k landslide. The model was calibrated using field data and results clarified characteristics about the extent and the depth of the landslide. Lo et al. (2014) examined the landslide occurring in the Dakeng bridge watershed at 115.9k of the Su-Hua highway and used PFC3D<sup>TM</sup> to model slope failure processes. From that model, the debris slide failure history and deposition characteristics of the slide were discussed.

Between Suao and Nanao on Route 9, the area most frequented by landslides is the Dakeng bridge watershed. Consequently, that portion of the highway is also frequently severed. Moreover, on October 21st, 2010, during

Typhoon Megi, the largest landslide on record for the watershed occurred. The volume of the landslide exceeded  $13,333 \text{ m}^3$  and caused the Suao to Dongao section of the Su-Hua Highway to be shut down for 25 days. Precipitation associated with storms following Typhoon Megi re-mobilized the landslide debris and caused additional deposition and aggradation of the stream channel. The stream bed aggradated to the point that it nearly crested the bridge. The elevated stream channel also allowed debris flows to flow against and scour the channel walls and in turn caused additional undercutting and failure of the adjacent slopes.

Due to the high risk slope instabilities at 115.9k of Route 9 posed to motorists, the MOTC decided to construct a new, larger bridge to increase the cross section for flood flows and reduce the risk associated with the debris flows and landslides. Image interpretation of the Dakeng bridge watershed has revealed fresh tension cracks along the edges of the watershed and the landslide bodies associated with those cracks are becoming increasingly unstable, indicating that the watershed will continue to be affected by debris slides. Resultantly, this study aims to clarify the future evolution of these unstable or gravitationally deformed areas and the possible effects of continued debris slides on Route 9. Using 1 m resolution LiDAR data collected via a Reigal LMS-Q680i scanner, the micro-topography of the landslide is interpreted and the extent of the gravitationally deformed areas associated with instability are identified. Then using an empirical formula for landslide volume based on the area, a volume representative of the volume that might result by failure of the gravitationally deformed areas is estimated. Finally, adopting PFC3D™, the failure process is modeled and the extent affected by the landslide, or run-out, is estimated.

## 2. Study area

The Dakeng bridge watershed is located in Suau township of Yilan County (indicated by the red square in Fig. 1). The west side of the area is the Central Mountain Range while the east side is the Pacific Ocean. Su-Hua highway is located at the foot of the mountains that border the Pacific Ocean. The topography is incredibly steep and the location of the road snakes through the coastline with the natural variations in topography. Much of the slopes are south, south-east facing. The study area extends from 115.8k to 116.4k of Route 9 and includes all of the Dakeng bridge watershed. The watershed has

an area of 30.5 ha and is divided by a dense network of streams. The average slope of the watershed is 41 degrees, with the highest slope being 63 degrees. The highest elevation in the watershed is 800m which is 900 meters horizontally from the junction of the highway and the watershed, which has an elevation of 270 m. The steep topography promotes highly erosive stream flow that during heavy rains, often cause landslides. In extreme cases the landslides transition into highly destructive debris flows, which in turn threaten Route 9. According to a 1/50,000 Central Geologic Agency map of the watershed, the watershed is comprised of an exposed section of Amphibolite within the Tungao Schist. The rock has a strike of N80W and a dip of 80 degrees to the south. The rock has a consistent orientation within the watershed. Although the strength of the Amphibolite is relatively high, the rock is heavily jointed and highly fractured.

The study area lies in a south Asia tropical monsoon climate which is characterized by heavy rainfall. Between 1971 and 2009, the average annual rainfall was greater than 4,480 mm. According to Central Weather Bureau records between 1971 and 2009, the hottest temperature occurs during July with an average of 32.0 degrees and the coldest temperature occurs in January, with an average of 12.9 degrees. The average number of rainy days is 210. Rainfall is heaviest during October to December. Every year, October to January is the northeast monsoon period. During that period, rainfall intensity is relatively low but duration is long. During the summer and fall, rainfall is intense and primarily due to typhoons.

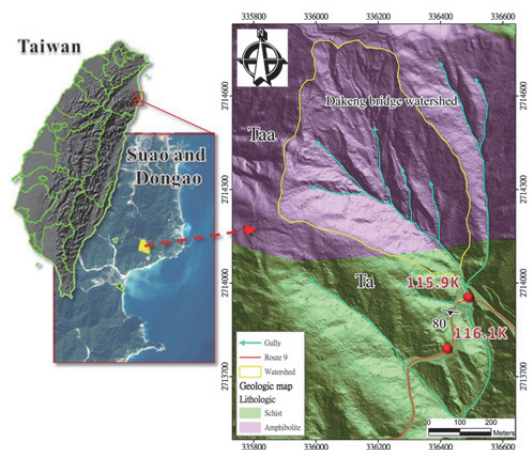


Fig. 1 Study location and geologic conditions (based on Central Geologic Survey 1/50,000 Taiwan geologic map for the Su-Hua area)

Table 1 Suao and Dongaoling weather station monthly average rainfall (CWB)

Month		1	2	3	4	5	6
Accumulated precipitation [mm]	Suao	364.9	339.7	211.2	192.8	267.4	248.8
	Dongaoling	687.8	659.3	328.0	215.0	797.0	363.5
Month		7	8	9	10	11	12
Accumulated precipitation [mm]	Suao	178.7	280.7	536.9	719.6	696.6	422.7
	Dongaoling	256.8	558.0	412.3	618.8	846.0	815.8

3. Methods

A flow chart describing the methodology the locations of unstable landslide bodies, predicting landslide volume and estimating the extent affected by the landslide is shown in Fig. 2. Micro-topography interpretation of LiDAR generated, high accuracy Digital Elevation Models (DEM) were used to identify the extent of the unstable, gravitationally deformed portions of the watershed. An empirical formula based on historic disaster records for landslide area and volume is then used to estimate the volume of material that may be generated by the gravitationally deformed areas. That volume is entered into a discrete element method model that is used to identify the area affected by the landslide.

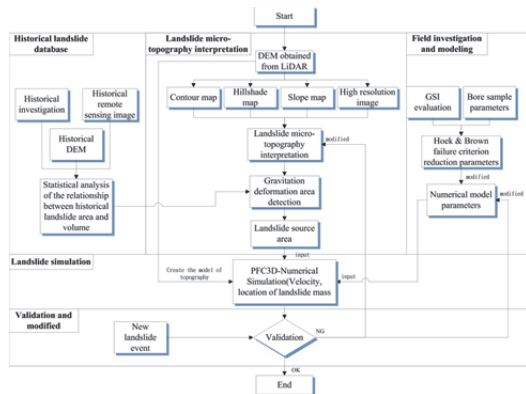


Fig. 2 Analysis flow chart of the study

3.1 Field investigation and modeling

Regarding numerical modeling, in addition to being heavily dependent on the model type and mesh, geotechnical parameters are also very important. Parameters that reflect the bedrock strength and deformability include the rock type, stratification, single compressive strength and deformation modulus. Usually, bedrock model parameters are obtained using physical experiments and published data and as a result are not necessarily representative. However, this study uses values recorded from the study area collected by the MOTC (Table 2, Figure 3) to select the parameter values for the model. Additionally, in order to account for the moderate to high degree of weathering and jointing observed in the exposed bedrock along the entire length of Suhua highway, the

compressive strength values from the MOTC survey, which were obtained from solid, un-weathered cores, are reduced using the Hoek and Brown failure criterion (Hoek et al., 2002). In that method, the compressive strength of the cores sample, Geologic Strength Index (GSI), rock characteristics and degree of disturbance are taken into account to estimate the reduced strength of the exposed bedrock. Based on field investigation, the mean GSI value in the study area was 50. Sample locations, bedrock conditions and the strength reduction parameter are shown in Fig. 4 and Table 3.

Table 2 Bore sample parameters (MOTC, 2012)

Core ID	Lithology	X(TWD97)	Y(TWD97)	Depth(m)	Unit weight (t/m <sup>3</sup> )	v
BT-07-02	Amphibolite	334640	2714397	96.12-96.25	3	0.1
Peak strength		Residual strength		Uniaxial compressive strength (Mpa)	Elastic modulus (Mpa)	
c(kg/cm <sup>2</sup> )	Ø (degree)	c(kg/cm <sup>2</sup> )	Ø(degree)			
-	-	0.00	25.5	68.6	33486.8	

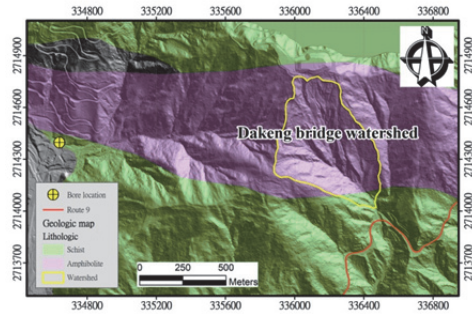


Fig. 3 Study area and location of borehole (MOTC, 2012)

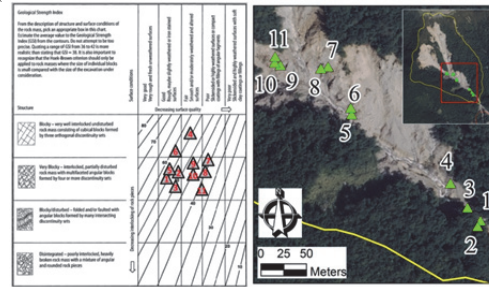


Fig. 4 The locations of GSI evaluation near Dakeng bridge

Table 3 Dakeng bridge watershed bedrock reduction parameters

Mean GSI	Rock type	Elastic modulus of intact rock (Mpa)	Revised elastic modulus from Hoek&Brown failure criteria E (Mpa)	Uniaxial compressive strength (MPa)	Unit weight (t/m <sup>3</sup> )	Angle of internal friction Ø	Rock lithology parameter mi	Disturbance factor D
50	Amphibolite	33,486.8	2,233.7	68.6	3.00	25.5	26	1.0

3.2 Historical sediment disaster records

To define a relationship between landslide area and volume, this study uses data reported by the MOTC Highway Disaster Information System, Fourth Maintenance Office of the Directorate General of Highways, Central Geologic Survey and Chou et al. (2012).

Additionally, the area of the unstable landslide bodies are identified using Suauo to Donao historical sediment disaster records and 2004 high resolution topographic data compared to 2011 high resolution LiDAR data collected by this study. We choice five areas of exposed bed rock by field investigation, which didn't had colluvium accumulation body on the slope. To ensure regression result is correct, and beside add more samples. The lost volume between 2004 to 2011 were selected (Fig. 5) to develop a landslide area and volume relationship. That relationship was then used to estimate the volume of sediment produced by unstable areas of the Dakeng bridge watershed (Table 4).

To ensure numerical model results are representative of field conditions, an empirical formula was developed based on historic landslide area and volume records and was used to estimate landslide volume. Chen et al. (2010) constructed landslide area and volume regression equations using remote sensing data of the Shihmen reservoir watershed, Also, Guzetti et al. (2009) and Korup (2005) developed power law regression equations based on landslide area and volume using landslides in Collazzone, Italy and the Southern Alps of New Zealand, respectively; the volume-area relationships were generally in agreement. In this study, a power law regression equation is developed using the landslide area and volume of 17 landslides that occurred near Route 9 to develop an empirical equation for landslide area and volume for landslides that occur between Suao and Donao along Route 9.

Table 4 17 landslides used to construct landslide area-volume regression equation

Landslide name	Source	Slope area(m <sup>2</sup> )	Landslide volume, (m <sup>3</sup> , loose material)	Landslide volume, in situ (m <sup>3</sup> )	Mean depth(m)
Hwy 9, 115.9k, (Area 1)	Comparison of two 2004 and 2011 DTM	6,572.9	-	44,326.6	7.40
Hwy 9, 115.9k (Area 2)		2,010.0		13,063.1	6.50
Hwy 9, 115.9k (Area 3)		2,668.1		20,275.9	7.60
Hwy 9, 115.9k (Area 4)		545.9		3,170.4	5.81
Hwy 9, 115.9k (Area 5)		773.0		5,169.5	6.69
Hwy 9, 115.9k	Chou et al., 2012	126,795.2		1,786,000.0	14.09
Hwy 9, 111.18k	CGB	1,495.6		714.0	0.48
Hwy 9, 124.27k		496.3		255.2	0.51
Hwy 9, 104.87k	Directorate General of Highways, Fourth Maintenance Office	1,822.2	1400.0	1,120.0	0.96
Hwy 9, 105k		495.3	1400.0	1,120.0	3.53
Hwy 9, 106.6k		1,834.9	6480.0	5,184.0	4.41
Hwy 9, 106.8k		2,548.6	1960.0	1,568.0	0.96
Hwy 9, 107.69k		154.2	50.4	40.3	0.41
Hwy 9, 109.1k		52.0	45.0	36.0	1.08
Hwy 9, 110.4k		635.7	3240.0	2,592.0	6.37
Hwy 9, 116.8k		346.5	2580.0	2,064.0	9.31
Hwy 9, 121.7k		644.2	2520.0	2,016.0	4.89

※The volumes reported by the Fourth Maintenance Office of the Director General of Transportation are loose material. According to the New Taipei Agricultural Department and Technology analysis manual(2011), 1 m<sup>3</sup> of in situ material is equal to 1.25 m<sup>3</sup> of loose material.

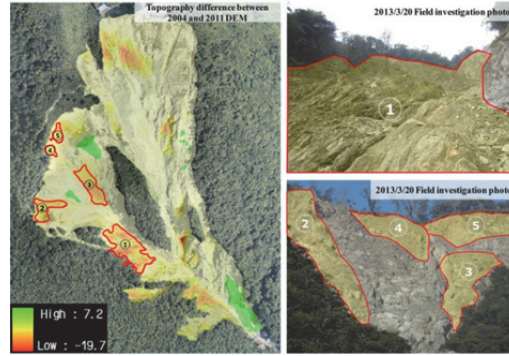


Fig. 5 Difference in 2004 and 2011 DEM in upper reach of the Dakeng bridge watershed and field photos. Positive signifies deposition; negative signifies reduced surface elevation.

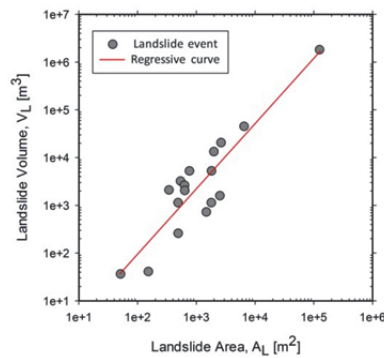


Fig 6. Power regression model constructed from historical landslide area and volume records of 17 landslides.

This study adopts a regression equation to estimate landslide volume based on landslide area (Fig.6). The R-squared value for the equation used is 81.9%, which demonstrates a significant exponential relationship. The optimal regression equation was found to be:

$$V_L = 0.1751 \times A_L^{1.3673} \quad (1)$$

where,  $V_L$  = landslide volume(m<sup>3</sup>) and  $A_L$  is the landslide area(m<sup>2</sup>). Equation (1) is used to convert that landslide area to a volume. This study uses micro-topography interpretation to identify the extent of gravitational deformation areas, which is assumed equal to the landslide area. Once the landslide volume has been determined, the numerical model is then run based on that value.







### 3.3 LiDAR Landslide micro-topography interpretation

The stability of a landslide body and the development of a potential failure surface are interrelated. If the landslide body is comprised of disturbed and loose material, the failure surface may develop within the body itself. There is an existing failure surface within the hillslope and deformation and displacement are

likely to occur. If the failure surface exists along a free surface outside of the landslide body, once the shear strength along the surface is smaller than the driving forces resulting from gravity acting on the landslide body, shear failure occurs (Baker, 1981; Sharma et al., 1995). Tension cracks, scarps and other linear features mark these types of failure processes and can be utilized to identify the extent of the failure surface (Agliardi, 2001; Chigira, 2009; Razak et al., 2009, 2011; Lopez Saez et al., 2012).

The gravitation deformation area is also surrounded by the linear landslide features. In the past, such linear landslide features were unidentifiable on slopes covered with dense vegetation. However, modern high resolution surveying techniques can now work around the vegetation. Moreover, while high resolution survey images are critical to successful landslide identification, the methodology used identify the linear landslide features in the images is also important. This study references features associated with gravitation deformation areas described in Soeters & van Westen (1996) and Chigira (2011)(Table 5) to identify the boundary of the gravitation deformation area in the Dakeng bridge watershed. The identified area is then entered into the landslide area-volume empirical equation to compute the probable landslide volume. That volume is then input into the numerical model to estimate the zone affected by the landslide. Interpretation of the gravitational deformation areas is shown in Fig. 7.

Table 5 Irregularities associated with gravitation deformation areas (From Soeters and van Westen, 1996; Chigira, 2011)

Irregularity	Description	Illustration
Step-like morphology	Step-like morphology usually forms after the landslide body has mobilized. Material upslope of the landslide scar moves downslope into the scar, forming the step like topography at the upper edge of the landslide	
Semicircular niches	Semicircular niches form in the head of the landslide.	
Back tilting of slope faces	The occurrence of back tilting slope faces indicates rotational failure. This feature is often oval or square in the horizontal surface and generally occurs in poorly drained material.	
Hummocky relief	Irregular topography that generally indicates instability and past movement and may be related to shallow failures or small failures moving towards an existing landslide scar.	
Formation of cracks	Fresh, open cracks that are evidence of recent movement and indicate the landslide body is sliding or tipping. Often the cracks parallel the edge of a scar.	
Steeping of slopes	Once the landslide has occurred, an over-steepened slope, or scar remains, severing the head of the landslide.	

Shaded relief generated from 2011 high resolution LiDAR data as well as aerial photos and a map shaded according to slope were used to perform topography interpretation. Identifiable linear features were recorded. From the map shaded according to slope, the location of linear, mobile areas is clear. From the two dimensional profile A-A' point 2 and 4 and profile B-B' point 6 and 8 show the over-steepening of slopes. Combined with aerial photos and the shaded relief topography, tension crack features at the head of the landslide are evident. These clues signify that the scar and head of the landslide are still mobile and within the gravity deformation area. The shaded relief map reveals mounds of material deposited at the foot of the hillslope that may have resulted from landslides at the top of the slope. The gravity deformation area is 59,560 m<sup>2</sup> and is shown in Fig. 8.

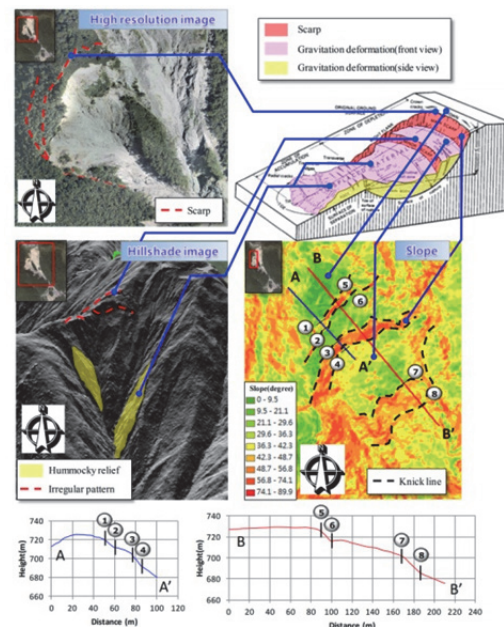


Fig. 7 Indications of gravitation deformation area. The number 1~8 is the location of slope map topographic profile.

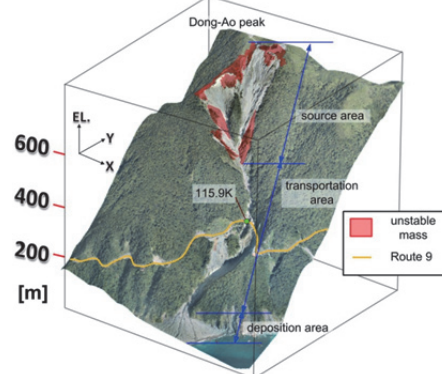


Fig. 8 Results of gravitation deformation interpretation

### 3.4 Numerical model

To estimate the area affected by failure of the gravitation deformation in the Dakeng bridge watershed, this study utilizes three dimensional discrete element method software, PFC3D™ (Lo et al., 2011 ; Chou et al., 2012 ; Lo et al., 2014). This software was developed by Itasca company in 1999 (Itasca, 2002) and primarily uses wall and ball shaped elements and the discrete element method to compute the change in location of each ball shaped element for each time step. In this way, the ball shaped elements are used to model the landslide body and the wall is used to model the failure surface. For each time step, the location and overlap amount or relative displacement is computed. Using the force-displacement law to estimate contact forces, Newton's second law of motion is applied using a model coefficient of friction. Once the force between the ball shaped element and the wall element exceeds the resistance force due to friction, the ball shaped elements begin moving, and in this way the velocity and position of each element are computed and the dynamic behavior of the mobilized landslide body as well as the area affected by the landslide are estimated. PFC3D™ utilizes the forces resulting at each contact point between elements to model the mechanics involved in the deforming material. Three types of contacts were used including stiff, smooth and bonded. Stiffness is computed assuming that the stiffness coefficient of the two neighboring particles is normal or in shear and interacts like a series of springs. Stiffness in the normal direction ( $k_n$ ) and the shear direction ( $k_s$ ) are described by equation (2)

$$k = \frac{k^{[A]}k^{[B]}}{k^{[A]} + k^{[B]}} \quad (2)$$

where, [A] and [B] are the two elements in contact,  $k$  is the normal stiffness( $k_n$ ) or the shear stiffness( $k_s$ ). The numerical model uses the aforementioned ball shaped elements in the PFC3D™ software to model the movement of the landslide body and the wall elements to model the intact, stationary bedrock boundary. Characteristics of the landslide material in the field are reflected in the model parameters using methods described in Potyondy and Cundall (2004):

$$k_n, k_s = 4RE \quad (3)$$

where,  $k_n$  is the normal stiffness,  $k_s$  is the shear stiffness,  $R$  is the radius of the model ball shaped elements (unit: m),  $E$  is the Young's modulus.

In consideration of computation time, a 5m x 5m DEM of the intact slope and surrounding topography were used for modeling.

The volume of the landslide was derived from the gravitational deformation area and the area-volume empirical relationship. The volume of the landslide body was determined to be 324,490 m<sup>3</sup>. To model this volume, 4,960 ball shaped elements, each having a radius of 2.5 meters were used as the landslide material. The topography of the model is based on the 2011 LiDAR DEM which was represented in the model by a total of 76,951 wall elements. Model conditions and parameters are shown in Fig. 9.

PFC3D™ model results reveal that most of the landslide material moves along the stream upstream of the Dakeng bridge (Fig. 10). The highest velocity attained during failure is 10 m/s and occurs as the landslide body drops from the top of the slope. As a result of the relatively large assumed volume of the landslide body, multiple zones of deposition form at the stream confluence with deposition depths as high as 13 m. Consequently, these results suggest that a landslide dam could possibly form near the confluence.

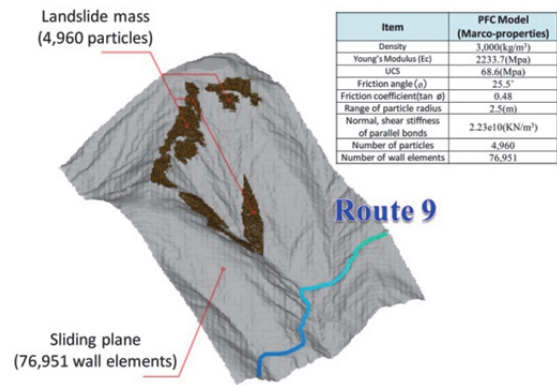


Fig. 9 Dakeng bridge watershed landslide model initial conditions

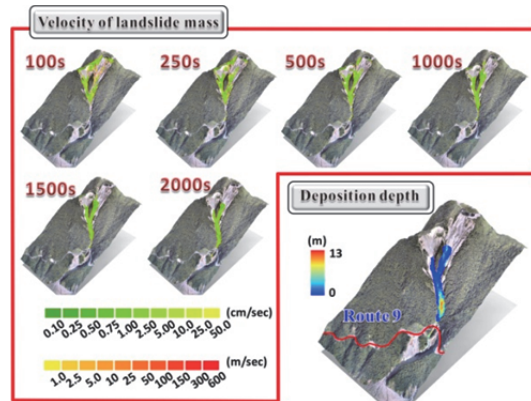


Fig. 10 PFC3D™ model results

## 4. Conclusion

Field examination of the Dakeng bridge watershed reveals that bedrock is generally high in strength but heavily fractured (GSI =50).

From interpretation of high resolution remote sensing data, it is evident that the north-west ridge boundary of the Dakeng bridge watershed is not only marked by many tension cracks but also has many areas of gravitational deformation. The area defined by these features is 59,560 m<sup>2</sup>. Historical hazard records were used to develop a landslide area to volume empirical model. Using this model, the volume of landslide material was found to be 324,490 m<sup>3</sup>, which was then input into PFC3D<sup>TM</sup>. Overall, the study area is a steep, convergent drainage. Stream flow is rapid and during high flows, colluvium and other landslide materials are entrained by the water and the erosive force of the stream is rapidly enhanced. In the future, in addition to monitoring the area downstream of the deposition zone (Route 9 115.9k to 116.1k), the banks of the stream that are actively eroded by the stream in the sinuous portion of the stream (approximately 115.8k - 116.4k) also need to be frequently examined. During typhoon rainfall, hazard response plans will need to be initiated.

## 5. Acknowledgements

This research is indebted for assistance and discussion on natural disaster investigation provided by C. M. Lo at Department of Civil Engineering, Chien-Kuo Technology University, and M. L. Lin at Department of Civil Engineering, National Taiwan University. Additionally, the authors thank Strong Engineering Consulting Co., Ltd. for providing the airborne LiDAR data (2011).

## References

- Agliardi, F. (2001): Structural constraints on deep-seated slope deformation kinematics, *Engineering Geology*, Vol. 59, pp. 83-102.
- Baker, R. (1981): Tensile strength, tension cracks, and stability of slopes, *Soils and Foundations*, Japanese Society of Soil Mechanics and foundation Engineering, Vol. 221, pp. 1-17.
- Chigira, M. (2009): September 2005 rain-induced catastrophic rockslides on slopes affected by deep-seated gravitational deformations, Kyushu, southern Japan, *Engineering Geology*, Vol. 108, pp. 1-15.
- Chen, S.C., Weng, K.L., Wu, C.H. (2010): The characteristics of landslides and landslide size in Yu-Fong river watershed, *Journal of Chinese Soil and Water Conservation*, Vol. 41(3), pp.217-229 (In Chinese)
- Central Geologic Bureau (2011): The report of disaster during Typhoon Megi along Route 9 between Suao and Dongao, Central Geologic Bureau.(In Chinese)
- Chigira, M. (2011): The Potential Area of Large-Scale Landslides (In Chinese), Scientific & Technical Publishing Co., Ltd: Taipei, Taiwan.
- Chu, H.K., Lo, C.M., Chang, Y.L. (2013): Numerical analysis of slope stability at the 115.9k point of the Su-Hua Highway. *Journal of Chinese Soil and Water Conservation*, Vol. 44(2), pp. 97-104.
- Chou, H.T., Lee, C.F., Lo, C.M., and Lin, Z.P. (2012): Landslide and alluvial fan caused by an extreme rainfall in Suao, Taiwan, 11th International Symposium on Landslides (ISL) and the 2nd North American Symposium on Landslides, Banff, Alberta, Canada.
- Directorate General of Highways (2012): The report of geological exploration services along Route 9 between Suao and Dongao. (In Chinese)
- Guzzetti, F., Ardizzone, F., Cardinali, M., Rossi, M., and Valigi, D. (2009): Landslide volumes and landslide mobilization rates in Umbria, central Italy, *Earth and Surface Science Letters*, Vol. 279, pp. 222-229.
- Hoek, E., Carranza-Torres, C.T., and Corkum, B. (2002): Hoek-Brown failure criterion-2002 edition, *Proceedings of the fifth North American rock mechanics symposium*, Vol. 1, pp. 267-273.
- Itasca Consulting Group Inc. (2002): PFC3D Particle Flow Code in 3 Dimensions. User's Guide. Minneapolis, USA.
- Korup, O. (2005): Distribution of landslides in southwest New Zealand, *Landslides*, Vol. 2, pp. 43-51.
- Lai, T. C. (1986): Study on the geotechnical property of rock masses along the Suhua Highway, and their engineering significance, *Bulletin of Central Geological Survey*, Vol. 4, pp. 55-102. (In Chinese)
- Lee, K.T. (2010): Analysis of disaster during Typhoon Megi along Route 9 between Mileage about 104K to 120K. (In Chinese)
- Lo, C. M., Lee, C. F., Chou, H. T. and Lin, M. L. (2014): Landslide at Su-Hua Highway 115.9k triggered by Typhoon Megi in Taiwan, *Landslides*, Vol.11, No. 2, pp. 293-304.
- Lo, C. M., Lin, M. L., Tang, C. L. and Hu, J. C. (2011): A kinematic model of the Hsiaolin landslide calibrated to the morphology of the landslide deposit, *Engineering Geology*, Vol. 123, pp. 22-39.
- Lopez Saez, J., Corona, C., Stoffel, M., Astrade, L., Berger, F., and Malet, J.P. (2012): Dendrogeomorphic reconstruction of past landslide reactivation with seasonal precision: the Bois Noir landslide, southeast French Alps,

- Landslides, Vol. 9, pp. 189-203.
- New Taipei Agricultural Department (2011):  
New Taipei Agricultural department and  
Technology analysis manual, New Taipei  
Agricultural Department. (In Chinese)
- Potyondy, D., and Cundall, P. (2004):  
Abonded-particle model for rock, International  
Journal of Rock Mechanics & Mining Sciences,  
Vol. 41, pp. 1329-1364.
- Razak, K.A., Straatsma, M.V., van Westen C.J.,  
and Malet J.P. (2009): Utilization of airborne  
LiDAR data for landslide mapping in forested  
terrain: status and challenges, Proceedings of  
the 10th South East Asian Survey Congress  
(SEASC), Bali, Indonesia.
- Razak, K.A., Straatsma, M.W., van Westen C.J.,  
Malet J.P., and de Jong S.M. (2011): Airborne  
laser scanning of forested landslides  
characterization: terrain model quality and  
visualization, Geomorphology, Vol. 126, No.  
1-2, pp. 186-200.
- Sharma, S., Raghuvanshi, T.K., and Anbalagan,  
R. (1995): Surface failure analysis of rock  
slopes, Technical Note, Geotechnical and  
Geological Engineering, Vol. 213, pp. 105-111.
- Soeters, R., and van Westen, C.J. (1996):  
Landslides: Investigation and Mitigation,  
Transportation Research Board Special Report,  
Vol. 247, pp. 129-177.